CHAPTER 4 MODEL DEVELOPMENT

4.1 Introduction and reviews

As mentioned in Chapter 2, the tendency of bed particles to agglomerate is influenced by several factors such as their physical and chemical characteristics, the characteristics of the ash, the reaction mechanisms and the collision among particles. It is directly proportional to the particle adhesive properties and to the area of contact and inversely proportional to the particle momentum [15]. Interparticle forces which associate to the particle agglomeration of fluidized bed include van der Waals force, liquid bridge force and viscous force [87]. The formed liquid/molten phase existing on the surface of the moving bed particles makes them to be more deformable and inertia, so the agglomeration is easily taken place during FBC/FBG as described by the viscous sintering. Agglomerate is formed as the momentum of the colliding bed particles, induced by the kinetic energy of fluidizing gas, is dissipated by the interparticle forces [82,109]. The agglomerates can meanwhile suffer the breaking when these forces inside agglomerate are defeated by the segregated force such as the gravitational force or collision force. Some solutions involve changing the operating conditions in the bed to avoid the adhesion together or using alternative inert bed material and adding additives to reduce the tendency.

The mathematical models have been developed to predict particle/bed agglomeration characteristics, such as the minimum fluidization velocity, the minimum sintering temperature, the defluidization time and the agglomeration size and growth, based on the different approaches. Several models employ the mass balance and force balance combined with the statistical regression analysis to complexly formulate, or are the simple empirical model. The formulas of agglomeration and defluidization are summarized in Table 4.1, viz;

Gluckman et al. [18] performed defluidization experiments using a number of bed materials and correlated the fluidizing gas velocities as a linear function of temperature above the initial sintering temperature (T_S). Below T_S, the bed can always be fluidized at minimum fluidization velocity, while above T_S, a correspondingly higher fluidization velocity was needed to fluidize the bed. The minimum fluidization velocity was no longer determined only by a balance of gravity, buoyant and drag force but the interparticle cohesiveness and particle kinetic energy had to be taken into consideration, when particles were fluidized at temperature above T_S. The bed height was an influence on the tendency.

Siegell [154] correlated the fluidization velocity data in term of the excess velocity needed to keep the bed fluidized at high temperature to the excess temperature relative to T_S in high temperature defluidization experiments with several particle materials. The linear relationship between these two parameters was found.

Compo et al. [155] measured the fluidizing air velocity during high temperature defluidization experiments with a wide range of materials. The dimensionless excess velocity was correlated with the dimensionless excess temperature relative to T_S observing both linear and non-linear relations, and classified these according to whether the solid was amorphous or crystalline.

Table 4.1 Models of agglomeration/defluidization

Author	Calculation object	Model	Description/Note
Gluckman et al. [18]	Minimum fluidization velocity at sintering conditions	$U_{mf,S} = B + AT$, at $T \geq T_S$	- Particle material dependent - T_S is defined as the temperature at intersection between the experimental U - T curve result and traditional U_{mf} - The linear relationship
Siegell [154]	Minimum fluidization velocity at sintering conditions	$U_{mf,S} - U_{mf} = f(T - T_S)$	- Particle material dependent - T_S is determined by dilatometry technique - The linear relationship
Compo et al. [155]	Minimum defluidization velocity[1]	$\frac{U_D - U_{mf,S}}{U_{mf,S}} = f(\frac{T - T_S}{T_S})$	- T_S is determined by dilatometer - Linear and non-linear behaviors were observed which was classified by amorphous or crystalline material - $U_{mf,S}$ was obtained by correcting measured U_{mf} at ambient for gas property changes
Basu [156]	The limiting velocity for defluidization (Dubbed as minimum fluidization velocity at sintering conditions)	$U_{mf,S} = \frac{1}{1650}\frac{d_p^2 g}{\mu_g}\left(\rho_p - \rho_g + \frac{\psi(T,H_b,d_p)}{1-\varepsilon}\right)$ $\psi(T,H_b,d_p) = K(T - T_S)f_1(d_p)f_2(H_b)$ where $T_s=f_3(d_p,H_b)$ and $f_3(d_p,H_b)$ $\Psi(T,H_b,d_p) = 0$ at $T \leq T_S$	- Adhesive force is included to **Ergan's equation** [148], as ψ force function - T_S of particle is determined by dilatometry experiments - Verified with the results of coal ash agglomeration experiment
Liss et al. [157]	Minimum fluidization velocity at sintering conditions	$Ga(1+Co) = 150\left[\frac{(1-\varepsilon_{mf})}{\varepsilon_{mf}^3}\right]\mathrm{Re}_p + \frac{1.75}{\varepsilon_{mf}^3}\mathrm{Re}_p$ $Co = f((T - T_S)/T_S),.....)$	- Adhesive force is included to **Ergan's equation** - A non dimensional function of Co was used to be established by the results of copper bead sintering [154]
Seville et al. [158]	Minimum fluidization velocity at sintering conditions	$\ln(U_{mf,S} - U_{mf})/H_{mf} = \ln(K_2/\alpha\eta_0) - \frac{E_{\mu,s}}{RT}$	- Based on visco-plastic sintering - Based on a comparison of characteristic times for quiescent motion of particle in bed and for the growth of sinter necks

Table 4.1 Models of agglomeration/defluidization (Continue)

Author	Calculation object	Model	Description/Note
Knight et al. [159]	Minimum bed breaking fluidizing velocity under sintering condition[2]	$U_{BB} - U_{mf} = \frac{r_a^3}{x_c^7} K_1 K_2(T) D_{0,S} \exp\left(\frac{E_S}{RT}\right)$ K_1 = either H_{mf}/α or $2d_b/3$ and $K_2(T) = 56\zeta\delta^4/kT$	- Based on diffusion sintering - Based on a comparison of characteristic times for quiescent motion of particle in bed and for the growth of sinter necks
Tardos et al. [160,161]	Limiting gas velocity[3]	$\frac{U_S - U_{mf}}{U_{mf}} = K\left[\frac{1-\varepsilon}{\varepsilon^2}\right]\left(\frac{d_{ag}^{7/4} d_b^{1/2}}{D_b^{1/2} d_p^{3/2}}\right)\left(\frac{\rho_g \sigma_S}{\phi \rho_s \mu_s g^{1/2}}\right)^{1/2}$	- Based on the force balance approach between the strength of agglomerates and forces resulting from bubble motion - Predicting in both low temperature condition by the presence of sticky liquid and high temperature sintering
Moseley et al. [162]	Minimum defluidization velocity[1]	$U_D = C_0 + C_3 \frac{((T/T_S)-1)^{5p}}{\left[1 - a(T-273)^b\right]^{2p}}$	- Employ a two particle collision model and a model for granular energy of the bed - T_S is determined by dilatometry technique
Yang et al. [163]	Agglomerate size distribution	$W(d_p,t) = W(d_p,t)\big\|_{t=0} + \frac{(Volume\_of\_agglomeration\_zone)}{(total\_weight\_of\_bed)} x \int_0^t Rate(d_p)dt$ $Rate(d_p) = \left\{ \sum_{\substack{d',d'' \\ d'+d''\to d_p}} f_{agg}(d',d'') - \sum_{\substack{d \\ d_p+d\to d'}} f_{agg}(d_p,d) \right\} x \left(\frac{\pi}{6} d_p^3 \rho_p\right)$	- In a cone shaped fluidized bed with a central gas jet - Based on the multi-phase hydrodynamic and heat transfer principles - Defluidization behaviors were excluded in the model.

Table 4.1 Models of agglomeration/defluidization (Continue)

Author	Calculation object	Model	Description/Note
Arena et al. [164]	Defluidization time	$t_{def} = \frac{1}{k(T)} \ln\left\{1 - \frac{\left\{\left[\left[0.5\exp\left(\frac{m_p u_0}{\mu_{pp}\pi r_p^2}\right) - 1\right] + 1\right\}^3 - 1}{\frac{Q_{pp}\rho_p / W_{bed}\rho_{pp}}{k(T)}}\right\}$	- The time is that the coating layer on bed particle reach to a critical thickness which dissipate the momentum of bed particle - Viscous flow sintering - Critical thickness is described by a critical stoke number (St) [165]
Lin et al. [109]	Defluidization time	$t_{def} = C\left(\frac{U - U_{mf}}{d_p}\right)^{1/2} \exp\left(\frac{E_\mu}{2RT}\right)$	- The time is that the coating layer on bed particle give adhesive force equal to breaking force induced by the passing bubble - Based on the coating induced agglomeration of K-silicates system and the viscous flow sintering
Lin et al. [166]	Defluidization time	$t_{def} = C\left(\frac{1}{f_N \psi}\right)\left(\frac{M^k}{d_p}\right)^{1/a} \exp\left(\frac{E_\mu}{RT}\right)$ $M = 0.67(1-\varepsilon_{mf})\rho_p\left(\frac{1}{\phi_b} - 1\right)(U - U_{mf})$ $\phi_b = \{1 - 0.3\exp[-8(U - U_{mf})]\}\exp(-\beta H_b)$ $\beta = 7.2(U - U_{mf})\exp[-4.1(U - U_{mf})]$	- Similar approaches with Lin et al [109] - The model of average convective solid mass flux [167] is employed as an expression of breaking force - Viscous sintering under Na species system

[1] Minimum superficial velocity is required avoiding defluidization under sintering conditions

[2] Dubbed alternatively, the minimum fluidization velocity is required preventing defluidization under sintering conditions

[3] Velocity is necessary to break the large agglomerates and to keep a bed of sticky particles fluidized at temperature exceeding T_S and/or if the bed contain a sticky material

Basu [156] and Liss et al. [157] modified Ergun's equation by including the adhesive force in the force balance. The expressions of minimum fluidization velocity under sintering conditions were derived as the adhesive force was correlated with the excess temperature with T_S. The models of Basu had been verified by the experimental results of the coal ash thermal sintering.

Seville et al. [158] compared two characteristic times to predict the defluidization velocity as the function of bed temperature, based on plastic viscous sintering; i) a time for which particles in the quiescent zone of fluidized bed remain in contact with others, and ii) a time for the growth of a neck between particles of sufficient size, and hence strength, to withstand the breaking force imposed by the movement of gas bubbles. Knight et al. [159] also employed this approach to develop a model based on the diffusion sintering.

A model of Tardos et al. [160,161] was developed to predict the limiting velocity to defluidize, based on the approaches viz; (i) the comparison between the breaking force acting on agglomerates and the agglomerate strength and; (ii) the equilibrium in the dynamic formation and break of agglomerates. In this model, the cohesive forces between granular was described by the presence of sticky liquids in both high and low temperature conditions and the bonding mechanisms between particles was associated to the liquid bridge, viscous sintering and high temperature sintering. The theoretical prediction and their results of experiments showed an exponential relationship between the dimensionless excess velocity and the dimensionless excess temperature, which was in an agreement with the data of Liss et al. [157] and Compo et al. [155].

Moseley et al. [162] proposed a kinetic model for calculation of defluidization velocity as dependence of temperature. It was suitable to viscous plastic sintering. The kinetic energy was taken to be dissipated in doing against an adhesive force on rebound. Two collision models and a model for the granular energy of the bed were used to formulate. They introduced a surface adhesiveness coefficient, which was early used by Liss et al. [157] as Cohesive number (Co), to account for the temperature effect.

Yang el al. [163] developed a model to predict the extent of agglomeration in a fluidized bed with a central jet. The model included mass and momentum balance to describe the fluid dynamics, and collision number and adhesive probability to describe the agglomerate rate. The defluidization phenomena were, however, excluded from the model.

Arena et al [164] calculated the predictive time at which defluidization occurred in plastic waste combustion. It was the time at which the viscous coating layer formed and extended by continuous plastic feeding reached to the critical thickness that had viscous resistance to bind together the two colliding particles within initial particle velocity. The condition for this defluidization limit, rebound occurs, could be described in term of a critical stoke number (St) [165].

In wheat straw combustion, Lin et al. [109] proposed a simple model of the breaking force, induced by bubbles, in linear function of the excess air velocity and an expression of the coating thickness relative to the combustion time and potassium content in linear function. The model was then developed based on the regression analysis to describe the defluidization time as a dependence of temperature, fluidizing velocity and bed

particle size, in an approach of the force balance between the strengthening adhesive by viscous sintering in the potassium silicate system and the breaking of fluidization.

Similarly, Lin et al. [166] also developed a predictive model of the defluidization time based on an approach of the adhesive-breaking force balance under the viscous plastic sintering of the sodium species system. A new expression of coating thickness relative to fuel properties and time was further applied and the model of average convective solid mass flux [167] was accounted as the expression of breaking force.

4.2 Modeling the bed agglomeration in FBC

In this work, the defluidization time of FBC defined as the predictive time at which the bed at specific operation conditions is reached to the complete defluidization state would be described by two present mathematical models. One was newly developed and another was a modified model based on the study of Lin et al. [109].

4.2.1 A presently developed model

1. Approach

The bed particles in the fluidized bed system keep moving, colliding, coalescing and breaking. After coalescence, agglomerates may also experience the strengthening or breaking. Based on these considerations as well as the present experimental results and discussion, which have been reported in the next chapter, the following assumptions were made:

- Defluidization is a result of competition between the total adhesive force in bed and the segregated force on agglomerates.
- Bed will be in the complete defluidization state when the total adhesive force equals, or exceeds, the segregated force.
- The segregated force on agglomerates is induced by the gas bubble.
- Bed agglomeration is caused by the formed melt fraction in the dominant potassium silicate system under the collision of melt transfer mechanism.
- Agglomerate is formed by the neck whose adhesive strength develops according to the viscous sintering mechanism and the melt induced agglomeration.
- Particles of bed material are sphere with uniform size.
- The ash content in bed increases linearly with combustion time.

2. Formulation

According to section 2.3.3, the size of the neck developed by the sintering therefore increases with time. In fluidized bed, the adhesion of two moving bed particles at u_p of each particles caused by a bonding neck of molten material at sufficient size was illustrated in Figure 4.1. Based on the information of sintering in Chapter 2, and applying a modified Reynolds lubrication equation [168] (Eq. 4.1) and Frenkel equation of viscous sintering [98] (Eq. 2.5), which described the viscous force of liquid bridge between two moving spheres,

$$F_{ad} = \frac{3}{2}\pi\mu_l r_p^2 \frac{1}{D} 2u_p \tag{4.1}$$

$$X^2 = \frac{3 \cdot r_p \cdot \gamma \cdot t}{2 \cdot \mu_l} \tag{2.5}$$

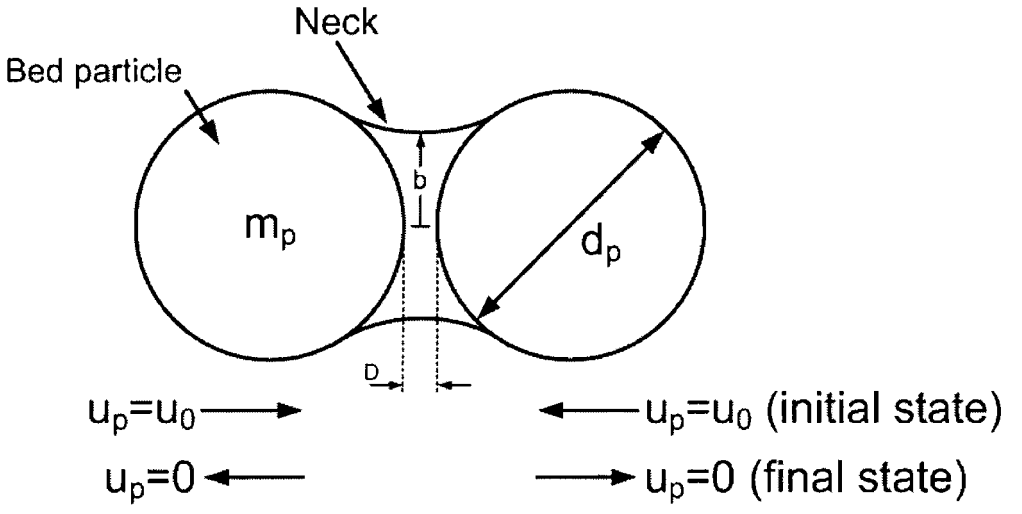

Figure 4.1 Illustration of adhesive force development by neck.

the adhesive force was herein simplified as;

$$F_{ad} = f(\mu_l, d_p, D, u_p, t) \tag{4.2}$$

where μ_l is viscosity of molten neck, d_p is particle diameter, D is particle separation distance, u_p is particle velocity and t is force developing time. The separation distance could be calculated from the kinematic law of Newton [169], also it was depended on;

$$D = f(\mu_l, d_p, m_p, u_p) \tag{4.3}$$

where m_p is the mass of a single particle. An average particle velocity (u_p) which represents the bed hydrodynamics depended substantially upon the bubble properties and was associated into the fundamental operating variables [148] viz;

$$u_p = f(d_b, d_p, S, u_b) \tag{4.4}$$

$$u_b = f(d_b, D_b, U) \tag{4.5}$$

$$d_b = f(\mu_g, \rho_g, \rho_p, D_b, H_b, U, U_{mf}) \tag{4.6}$$

$$S = f(d_b, u_b, U) \tag{4.7}$$

where ρ_g is the air density, ρ_p is the bed particle density, μ_g is the viscosity of air, d_b is the bubble diameter, D_b is the bed column diameter, H_b is the static bed height, S is the bubble separation length, u_b is the air bubble velocity, U is the superficial air velocity and U_{mf} is the minimum fluidization velocity.

In combination of Equation 4.2-4.7, the adhesive force per neck (F_{ad}) could be associated resultantly with the basic variables;

$$F_{ad} = f(\mu_g, \mu_l, \rho_g, \rho_p, d_p, D_b, H_b, m_p, U, U_{mf}, t) \tag{4.8}$$

The bed of inert particles at a specific experimental condition was partially and progressively defluidized by the thermally generated molten fraction of the inorganic constituents in biomass fuels, continuously fed during the steady state combustion. The complete defluidization was reached at the defluidization time (t_{def}), at which the adhesive force of a number of necks in bed was overcome by breaking force. Therefore, the total adhesive force ($F_{ad,total}$) at complete defluidization state was established;

$$F_{ad,total} = f(\mu_g, \mu_l, \rho_g, \rho_p, d_p, D_b, H_b, m_{bed}, m'_{fuel}, U, U_{mf}, X_{melt}, \%ash, t_{def}) \quad (4.9)$$

where X_{melt} is the melt fraction of ash in bed. It could be estimated from the phase diagram of involved ash elements in agglomeration by applying the "Lever rule" analysis [24], as mentioned in Appendix A, on the simplified initial fuel ash compositions at the surface temperature of the burning char particle. The char surface temperature was calculated according to the procedures in Appendix B. %ash is the percentage by weight of ash in biomass fuel on "as fired" basis. m_{bed} and m'_{fuel} are the bed inventory and fuel feed rate, respectively. X_{melt} and char temperature herein described an adhesive property of ash constituents.

Unfortunately, no exact mathematical model was published to describe the segregated force in fluidized bed. However, several pervious studies [108-109,164,170] suggested that the segregated force was defined from the behaviors of gas bubble in fluidized bed. Therefore, the segregated force of the present model was also correlated to the bubble properties in fluidized bed;

$$F_{seg} = f(d_b, S, u_b) \quad (4.10)$$

similarly simplified as;

$$F_{seg} = f(\mu_g, \rho_g, \rho_p, D_b, H_b, U, U_{mf}) \quad (4.11)$$

Defluidization time (t_{def}) was obtained by the setup in equality of Equation 4.9 and 4.11 as shown in Equation 4.12.

$$t_{def} = f(\mu_g, \mu_l, \rho_g, \rho_p, d_p, D_b, H_b, m_{bed}, m'_{fuel}, U, U_{mf}, X_{melt}, \%ash) \quad (4.12)$$

By mean of the dimensionless analysis, Buckingham-π theory [171], the variables in Equation 4.12 were grouped into the dimensionless terms;

$$\frac{m'_{fuel} \cdot t_{def}}{m_{bed}} = f\left(\frac{\mu_l}{\mu_g}, \frac{U}{U_{mf}}, \frac{d_p}{D_b}, \frac{H_b}{D_b}, (\%ash * X_{melt})\right) \quad (4.13)$$

The analysis of Multiple Linear Regression (MLR) on the lab scale experimental results was carried out in order to complete Equation 4.13 into general form of MLR model

(Equation 4.14), where B0 to B5 were the proportional constant, and to obtain the contribution of each independent dimensionless variable.

$$\left(\frac{m'_{fuel}.t_{def}}{m_{bed}}\right) = B0 * \left(\frac{\mu_l}{\mu_g}\right)^{B1}\left(\frac{U}{U_{mf}}\right)^{B2}\left(\frac{d_p}{D_b}\right)^{B3}\left(\frac{H_b}{D_b}\right)^{B4}\left(X_{melt}\%ash\right)^{B5} \tag{4.14}$$

Equation 4.14 was a purely statistical model. The viscosity ratio and melt fraction group represented the influence of fuel ash compositions and temperature on bed defluidization while the effect of bed hydrodynamics was described by the dimensionless velocity, particle size and static bed height. In this model, the viscosity of the molten ash (μ_l) was easily calculated from the practical viscosity model of the silicate glass melt [172] at the fuel ash composition and bed temperature. The gas properties were based on the physical properties of the air. It should be noted that although the present experiment was carried out with only quartz bed material, the effect of bed materials could have been physically taken into account in U_{mf} determined by Ergan's equation, as the bed particle density (ρ_p).

4.2.2 A modified model

A second model proposed in this work was modified from the model of Lin et al. [109] in order to probably correct the accuracy in the predication. The fully understanding of the model formulation and application in origin was thus necessarily.

1. Original assumption

Repeatedly, an original model [109] was early developed on the approach of the adhesive-breaking force balance. The adhesive force was well defined from the bonding stress on the neck cross sectional area as shown in Figure 4.2, while the breaking force was defined in the linear dependence with the excess velocity ($U-U_{mf}$). A linear extension of the coating thickness relative to the combustion time and potassium content in biomass was established and included in the model formulation. The assumptions of this formulation were as followed;

- The agglomeration tendency is caused by the formation of a coating layer composed of potassium silicates.
- Particles of bed material are spheres with uniform size.
- The coating is equally distributed on each sphere.
- The ash content in the bed increases linearly with time.
- Agglomerates are formed by necks, whose strength develops, according to the visco-plastic sintering mechanism.
- Defluidization is a result of competition between the adhesive force and the breaking force on agglomerates.
- The segregated force on agglomerates is induced by bubbles and is proportional to the excess fluidization velocity.
- If the adhesive force is equal to or higher than the breaking force, the bed will defluidize.

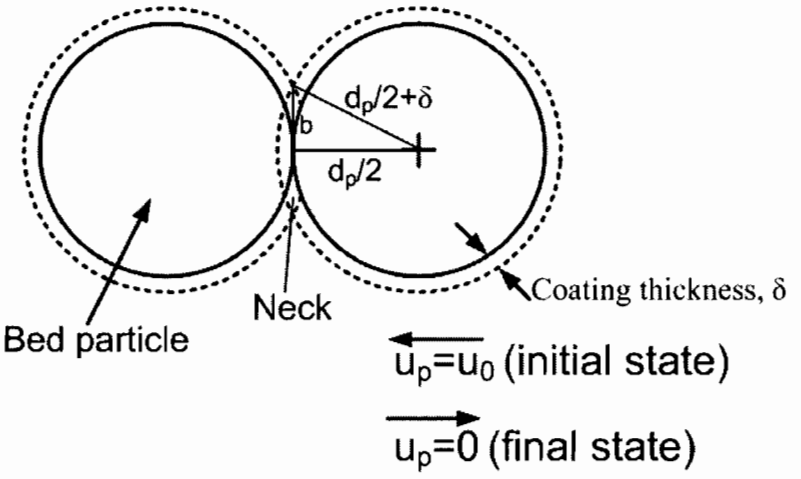

Figure 4.2 The development of adhesive force by bonding neck of coating [109].

2. Early formulation

The adhesive force between two particles caused by bonding, as illustrated in Figure 4.2, was described by

$$F_{ad} = \pi b^2 \sigma_S \tag{4.15}$$

where σ_s is the bonding stress. The accumulation of ash in the bed contributed to the build up of the coating and neck. According to mass balance and assumption, the thickness of coating layer on the bed particle as a function of time was expressed as;

$$n\rho_{coat}\pi d_p^2 \delta = C_1 m'_{fuel} X_{K-Fuel} t \tag{4.16}$$

where n is the number of bed particles, ρ_{coat} is the density of coating material, δ is the thickness of coating, $X_{K\text{-}Fuel}$ is weight fraction of potassium in the fuel and C_1 is the proportional constant. From Figure 4.2 and Equation 4.16, the growth of neck radius (b(t)) with the substitution for n was expressed as;

$$b^2 = d_p \delta = \frac{C_1 m'_{fuel} X_{K-Fuel} d_p^2 \rho_p t}{6 m_{bed} \rho_{coat}} \tag{4.17}$$

The strength development is proportional to the time and inversely proportional to viscosity of the coating due to the viscous sintering mechanism. The tensile stress of agglomerate (σ_S) was thus defined by [123];

$$\sigma_S = \frac{C_2 t}{\mu_l d_p} \tag{4.18}$$

where μ_l is the viscosity of coatings. Substitution of Equations 4.17 and 4.18 into 4.15, the adhesive force could be express as;

$$F_{ad} = \frac{C_3 d_p t}{\mu_l} \tag{4.19}$$

where

$$C_3 = C_1 C_2 \frac{\pi m'_{fuel} X_{K-Fuel} \rho_p}{6 m_{bed} \rho_{coat}} \tag{4.20}$$

The viscosity is dependent upon the composition and temperature in a K-Si system and the viscosity model applied was estimated by an Arrhenius's expression [158] as shown in Equation 4.21.

$$\mu_l = \mu_0 . \exp\left(\frac{E_\mu}{RT}\right) \tag{4.21}$$

where E_μ is activation energy of surface viscosity and μ_0 is pre-exponential factor for viscosity. The breaking force was assumed to be induced by bubbles and was proportional to the excess air as;

$$F_{br} = C_4 (U - U_{mf}) \tag{4.22}$$

When adhesive force (F_{ad}) is equal to the separating force (F_{br}), the bed is defuidized. Equations 4.19-4.22 were applied to obtain the defluidization time viz;

$$t_{def} = C\left(\frac{U - U_{mf}}{d_p}\right)^{1/2} \exp\left(\frac{E_\mu}{2RT}\right) \tag{4.23}$$

where

$$C = \sqrt{\frac{\mu_0 C_4}{C_3}} \tag{4.24}$$

3. Present modification

It had been noticed in Equation 4.24 that the fuel feed rate (m'_{fuel}), bed inventory (m_{bed}) and potassium mass fraction in fuel ($X_{K\text{-}Fuel}$) were considered to be the constant, and included in C constant. In present work, the effect of different biomass and bed conditions with one bed material were studied experimentally on the bed agglomeration tendency. The bed inventory, fuel feed rate and potassium content were therefore considered to be the variable, while the bed particle density (ρ_p) was considered to be the constant.

To obtain more generalized expression, the fuel feed rate, potassium content and bed inventory involved in C constant were separated out of Equation 4.24 and the equations were rewritten as,

$$t_{def} = C_{new}\left(\frac{m_{bed}}{m'_{fuel}\, X_{ash} X_{K.in.Ash}}\right)^{A}\left(\frac{U - U_{mf}}{d_p}\right)^{1/2} \exp\left(\frac{E_\mu}{2RT_b}\right) \quad (4.25)$$

where

$$C_{new} = \sqrt{\frac{6C_4\mu_0\rho_{coat}}{\pi C_1 C_2 \rho_p}} \quad (4.26)$$

where C_{new} and A were the presently defined constants. The original value of A was 0.5 [109] (Eqs. 4.20 and 4.24), while it expects to be 1 in this work. $X_{K\text{-}Fuel}$ was presented in the form of mass fraction of ash in the fuel (X_{ash}) and mass fraction of potassium in the ash ($X_{K\ in\ Ash}$). C_{new}, A, and E_μ would be calculated by the regression analysis on a set of present lab scale experimental data at constant air velocity and particle size. It was further noticed that the density of molten coating (ρ_{coat}) which was included in C_{new} (Eq. 4.26) was particularly depended upon the chemistry of coating material and the temperature, in a minor extent [173]. E_μ was also a function of the chemical composition of coating.

$$C_{news} = f(\rho_{coating}) \quad (4.27)$$

$$\rho_{coating}, E_\mu = f(the\_coating\_compositio n) \quad (4.28)$$

Therefore, these two parameters (C_{new}, and E_μ) could be possibly correlated as a function of the initial fuel ash composition, to which the coating composition was directly related.

Finally, the proposed models in Equations 4.14 and 4.25 were verified, in term of the defluidization time, with the present laboratory scale and pilot scale experimental results as well as the previous published experimental data.